Self Heating Under RF Power in BAW SMR and Its Predictive 1D Thermal Model

N.B. Hassine[1,2,3,*], D. Mercier[2], P. Renaux[2] , D. Bloch[2], G. Parat[2], B. Ivira[2], P. Waltz[1], C. Chappaz[1] , R. Fillit[4] and S. Basrour[3]

[1]STMicroelectronics, 38926 Crolles Cedex, France

[2] CEA-LETI/MINATEC, DRT/DIHS, 17 Rue des Martyrs, 38054 Grenoble Cedex, France

[3] TIMA CNRS-UJF-INPG Micro-Nano-Systems Group, 46 Avenue Félix Viallet, 38031 Grenoble Cedex, France

[4]Ecole Nationale Supérieure des Mines de Saint-Etienne, Saint-Etienne, France

Abstract— **This paper intends to provide a contribution for a better understanding of the self-heating effect in BAW SMR by developing a predictive 1D-model. Knowing the power dissipated inside the SMR, the presented model allows us estimating the temperature distribution inside the different layers of resonators used to build BAW filters. Model is compared with both experimental measurements and Finite Elements Analysis. Conclusions concerning the device reliability can eventually be drawn.**

I. INTRODUCTION

Nowadays, the Bulk Acoustic Wave (**BAW**) technology is demonstrated to be a well-suited candidate for Radio Frequency (**RF**) filtering applications [1]. However, despite many years of research and development and the great technological progress achieved till today, some domains are not satisfactorily understood and need to be thoroughly studied such as reliability which still requires complex analysis tools and testing protocol. One of the important points impacting the device reliability is the self-heating of BAW resonator under large **AC** signal and the increase of its internal temperature [2]. It may result in an undesirable functionality and even affect irreversibly the final product, especially in the case of the transceiver path of filters (**Tx**) expected to handle an incident power of 29 dBm maximum as for instance in **PCS** duplexer [3]. Even if BAW technology has better handling abilities compared to surface technology (**SAW**) mainly because electrical currents distribute more evenly, the tendency toward reducing the device size while keeping the same input power P_{in} leads to drastically increase the power density inside the filter. Accordingly, power handling capability issues arise and limits to the allowable input signal level can be reached. Furthermore, the BAW frequency shifts down when the device is heated up because of the negative temperature coefficient of frequency (**TCF**) [4]. So it is necessary for an accurate design of BAW filters operating at high signal level to model high power effects on the electrical response of the device. In this context, the present paper aims to contribute for a better understanding of the thermal behavior of BAW Solidly Mounted Resonator (**SMR**) [1] operating at high power level. To do it, a 1D-predictive model funded on the "cascaded" thermal resistance of each layer is developed.

*: corresponding author: nizar.ben-hassine@cea.fr

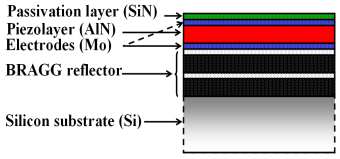

Figure 1. Simplified cross section of the BAW SMR device

After having determined the power dissipated inside the device P_d, the presented model allows estimating the maximum temperature T_{max} and the temperature distribution inside the SMR stack used to implement BAW filters. The Model results are compared with the experimental measurement realised with a high spatial resolution Infrared (**IR**) camera and Finite Elements Analysis (**FEA**) computed with ANSYS thermal analysis. The comparison of SMR performances with two different acoustic reflectors used for this technology is given and conclusions concerning the reliability of the final device are drawn.

II. DEVICE DESCRIPTION

The SMR basic structure is a piezoelayer sandwiched between two thin electrodes (Aluminium Nitride (**AlN**) and Molybdenum (**Mo**) respectively in our case). The resonator active part is mounted on a Bragg reflector deposited onto silicon substrate. The Bragg reflector is composed of a succession of quarter wavelength layers of high and low acoustic impedance [1], W and SiO_2 or SiN and SiOC respectively, for a targeted resonance frequency f_s of 2 GHz. This combination results in a high coefficient of reflection and consequently a better confining of the acoustic energy in the resonator active part. A SiN passivation layer is added above the stack to protect the SMR *(FIG.1)*.

III. THE THEORETICAL STUDY

The purpose of the present work is to give a simple thermal model that formulates in the best way the maximum temperature and the temperature variation inside the stack as a function of P_d and the stack technology. Along this study, the resonator is supposed in the steady regime. Furthermore, because of the structure symmetry and the isotropy of thermal coefficients in the *XY* plan, it is reasonable to consider a 1D model. The bottom substrate temperature

978-1-4244-3510-4/09/$25.00 ©2009 IEEE

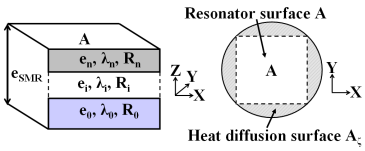

Figure 2. SMR multilayer stack, the top view and the coordinate system

T_{bottom_Si} is set to the ambient temperature T_{amb}=20°C**.** To define properly the heat source it is important to understand the heat generation phenomena in the SMR. For piezoelectric applications, the heat is generated due to dielectric loss, mechanical loss and the Joule effect. The dielectric loss in the piezolayer is considered as the main effect. Nevertheless, the Joule effect in electrodes can be not negligible especially at the resonance frequency [5]. As a consequence, the heat source in a SMR is its active part. In its simplest form, the SMR can be considered as a system of n layers with the same area A, an individual thickness e_i, a thermal conductivity λ_i and a thermal resistance R_i where the subscript i denotes the layer number and is ranged from 0 to n *(FIG.2)*. A first model allowing the calculation of the SMR equivalent thermal resistance R_{SMR} and the maximum temperature variation $\Delta T_{max} = T_{max} - T_0$ as function of P_d was suggested by taking into account the device area and approximating R_{SMR} by the substrate thermal resistance [6]:

$$\Delta T_{max} = R_{SMR} P_d \quad \textbf{(1)} \quad \text{and} \quad R_{SMR} \approx \left(\pi \lambda_{substrate} \sqrt{A}\right)^{-1} \quad \textbf{(2)}$$

This model gives a good estimation of T_{max} if the substrate has a high thermal resistance (as it is the case for the glass substrate λ_{glass}=1.04W/K.m) since the thermal resistance of the other layers is negligible [6]. However, this hypothesis can not be applied for SMR built onto silicon substrate, since the silicon thermal conductivity is much higher and some dielectric materials used in the Bragg reflector have a very high thermal resistance such as SiOC and SiO_2 (*TABLE-1*). Consequently, an accurate estimation of R_{SMR} needs to consider all SMR layers. Furthermore, it is well-understood that the higher the layer thickness the higher will be its impact on the overall thermal resistance. This is also an effect not considered in the previous model. For such a reason a thickness factor is defined for each layer with reference to the stack total thickness e_{SMR}:

$$\alpha_i = e_i / e_{SMR} \quad \textbf{(3)}$$

Moreover, since the heat diffuses in an isotropic way in the *XY* plan, it is more judicious to define the heat surface as the circumscribed circle ζ *(FIG.2)* rather than the resonator square with $A_\zeta / A = \pi / 2$. Thermal resistances are additive when they are in series, so R_{SMR} is the sum of individual thermal resistances multiplied by thickness factors:

$$R_{SMR} = \sum_{i=0}^{n} \alpha_i R_i = \frac{1}{e_{SMR}} \sqrt{\left(\frac{2}{\pi^3 A}\right)} \left(\sum_{i=0}^{n} \frac{e_i}{\lambda_i}\right) \quad \textbf{(4)}$$

This general relation should be used in the equation ***(1)*** to calculate T_{max} of a SMR if we need to consider all layers. The model enables also the comparison of different BAW stack performances from a thermal point of view and to take into account the geometrical parameters of each layer.

Layer:	Mo	AlN	SiO_2	W	SiN	SiOC	Si
e_i (µm):	0.25	1.25	0.75	0.65	1.13	0.325	725
λ_i (W/m·°C)	142	285	1.4	174	25	0.3	160
ρ (kg/m³)	10280	3280	2200	19250	2600	2100	2330
α (10^{-6}/°C)	5	4	0.5	4.5	3	15	2.5
E(GPa)	329	305	70	410	280	78	165

TABLE I. DATA FOR MODEL AND THERMAL SIMULATIONS

Next, it is interesting for a reliability study to know the temperature profile inside the structure. According to thermodynamic laws, the heat generated in the active part will be transferred inside the SMR in order to reach the thermodynamic equilibrium and consequently will modify the device internal distribution of temperature. To study the temperature variation along the Z-axis, it is necessary to estimate the significance of different heat transport mechanisms in the SMR stack. In general, the heat can be transferred between system parts by conduction, radiation and convection [7]. In the case of solids, the conduction is the most significant means of heat transfer [7]. For the SMR study, free convection and radiation fluxes are verified to be negligible compared to conduction flux in the expected range of temperature variation. As a consequence, the SMR thermal problem can be reduced to a heat source in series with several thermal resistances undergoing a conduction heat flux. According to the Fourier's law for the heat transfer, the conduction heat flux is given by:

$$Q_{conduction} = \Delta T / R_i \quad \textbf{(5)}$$

where ΔT is the difference between bottom and top layer temperatures and R_i is the thermal resistance of the layer [7]. Since the structure is made from materials of different thermal conductivities, it is recommended to use the thermal-electrical analogy to solve easily the problem. In such analogy, the thermal resistance, the temperature and the heat flow (which corresponds to P_d) are equivalent to the electrical resistance, potential and current respectively. The SMR electrical analogy is shown in *FIG.3*. Hence, it is straightforward to deduce the top and bottom temperature of each layer knowing P_d, T_{max} and R_i from the active part up to the layer of interest. As an example, if we consider a SMR with a four-layer Bragg stack (couple of SiOC and SiN layers), according to data given in *TABLE-1*, the overall thermal resistance $R_{SMR} \approx 23.7°C/W$ so for P_d=1W, ΔT_{max} is 23.7°C. In this case, the top substrate temperature is $T_{top\_Si} \approx 35.6°C$. If the Bragg consists of a couple of SiO_2 and W layers, $R_{SMR} \approx 19.5°C/W$ so for P_d=1W, ΔT_{max} is 19.5°C.

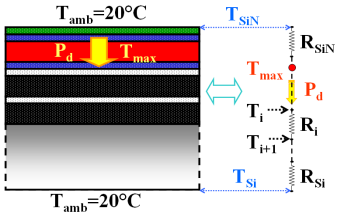

Figure 3. Thermal-electric analogy for the SMR problem

As consequence, for a given P_d, the SiO_2/W-SMR heats less than the SiOC/SiN-SMR (by about 20% of the total variation).

Once the analytical model is established, it is important to compare model results with the experimental measurement carried out in SMR devices and other tools usually used to solve similar problems such as Finite Elements simulations.

IV. Temperature Mapping with Infrared Imaging:

The goal of this part is to determine experimentally the resonator maximum temperature for a given P_d and SMR technology. A key point for such a measurement is to assess accurately P_d by measuring accurately P_{in} at the input of the resonator and the reflected power P_r since P_d is deduced from a power balance as follows:

$$P_d = P_{in} - P_r \quad \textbf{(6)}$$

At low P_{in} level (≤14dBm), this is easy to do through the well-known Scattering **(S)** parameters measurement. However, at high power level (P_{in} ≥20dBm), S parameters measurements are complex to perform and require important precautions especially if the studied device is highly sensitive to the frequency and temperature changes as the SMR. Furthermore, dedicated equipments are expensive and uncommon in RF laboratories. For such reasons, a measurement bench using current RF apparatus is presented here to measure P_d for a 1 port SMR *(FIG.4)*. The RF generator is connected to a variable gain power amplifier (**PA**) that increases the delivered signal. The amplified signal feeds the SMR via the circulator and the RF probe. A coupler is used to measure P_{in} via a first wattmeter. P_r is sent by the circulator to the second powermeter. Isolator is used to protect the PA while attenuators are used to keep powemeters input powers close to 0dBm for measurement accuracy. The whole setup test bench is computer monitored through GPIB. The measurement procedure consists of submitting the on-wafer SMR to RF signal with a variable frequency around f_s and the antiresonance frequency f_p at a fixed P_{in} to detect the frequency f_{max} that corresponds to the maximum of P_d. After that, the signal frequency and level are kept constant while a high resolution infrared camera is used to obtain an accurate temperature mapping of the studied device after the emissivity correction. Moreover, an optic zoom is used to enhance the spatial resolution up to 2µm/pixel and to allow infrared imaging at room temperature [2]. The self-heating of a SiN/SiOC-SMR and the temperature distribution in the surface for P_d=1.28W is shown in *FIG.5*. In this case, ΔT_{max}= 20.2◦C. According to the presented model, T_{max}= 30.3°C when P_d=1.28W which can be considered as a good estimation of the

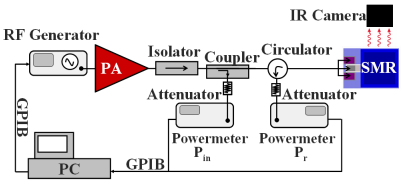

Figure 4. Setup for high power level characterization

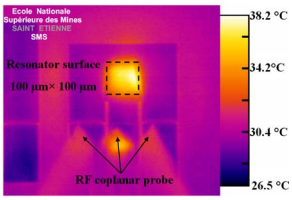

Figure 5. SMR Thermal imaging for P_d=1.28 W and A= 100 × 100 µm^2

experimental result. It is important to note in *FIG.5* that the heat diffuses largely in the surface surrounding the resonator certainly due to the high thermal conductivity of the AlN deposited on full-sheet. This heat spreading cools down the active part of the resonator and is the main explanation for the difference between experimental and model results. Moreover, the main heat surface diffusion looks a circle-like around the resonator square due to the isotropy in the XY plan as it was supposed in the developed model.

V. Finite Elements Modeling

A common method used to predict thermal performances is the Finite Elements Analysis (**FEA**). In this work, FEA is carried out for SMR in the steady-state regime in order to assess T_{max} versus P_d, to visualize the temperature distribution inside the SMR and to compare the thermal behaviour of the two Bragg technologies. This enables also to compare the computer simulated results with model and IR thermography results. ANSYS Multiphysics Workbench is used as FEA tool for this purpose. The simulated structure is given in *FIG.6-a*. The dissipated power density is entered as a uniform volume heat generation rate in the active part. A square resonator of $A=(100\mu m)^2$ is considered as in the measured SMR while the substrate lateral dimension is 1mm and its thickness is 725µm. SiN/SiOC and W/SiO_2 quarter wave length Braggs are simulated respectively and compared for the same P_d. All layers are taken full sheet except the top electrode and the passivation layer with the same material properties and thicknesses as given in *TABLE-1*. Since P_d is defined as a power density in the active part, two bodies are defined for both bottom electrode and piezolayer to apply the power density only in the resonator part. For heat transfer boundary conditions, radiation and free convection are taking into account in simulations and the substrate bottom is set to T_{amb}. Thanks to the structure symmetry, the quarter of the structure can be simulated to avoid heavy calculations.

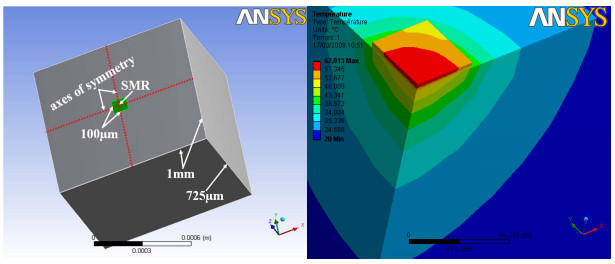

Figure 6. (a) The full simulated structure, (b) Simulated temperature distribution for SMR on SiN/SiOC bragg, T_{max} =62°C when P_d=1W

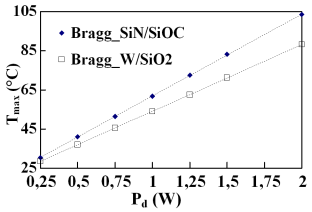

Figure 7. SMR T_{max} versus P_d for two BRAGG technologies

Consequently, heat flows are set to zero at symmetry plans. To obtain an accurate solution, a fine meshing is used for resonator layers and close regions in the substrate. A typical result of the temperature distribution is shown in *FIG. 6-b*. Radiation and free convection are verified to be negligible in our case even if large values for convection and emissivity coefficients are used. The highest temperature is located inside the active region and ΔT_{max}=42°C can be reached inside the SiN/SiOC-SMR for P_d=1W. The Bragg dielectric thickness (SiOC and SiO_2) is verified to be the most influencing parameter in the SMR stack. This is due to their high thermal resistances that make the active part more or less thermally isolated from the heat sink and hence T_{max} increases or decreases quickly. When plotting T_{max} versus P_d for the two different Bragg technologies *(FIG.7)*, T_{max} varies linearly versus P_d. This result is expected since nonlinear phenomena like temperature-dependent material properties and radiation are negligible for the studied problem. The slope of T_{max} versus P_d curve is higher in the case of SiN/SiOC Bragg than the SiO_2/W Bragg one. This means that the thermal resistance of the SiN/SiOC Bragg is higher than the SiO_2/W one which agrees with the model result. A difference of 10°C between the two structures is obtained in simulations when P_d=1W. In the other hand, simulation results are higher than the measured temperature. It is noticed that the temperature decreases quickly in the lateral directions in the case of simulation unlike the experimental measurement. This is likely the most important reason for the temperature difference. Another reason that can contribute to the temperature difference is the difference between the simulated structure and the real one.

VI. DISCUSSION AND CONCLUSION

Along this study, a thermal model based on the thermal conductivity of different layers constituting the SMR device is developed after the discussion of important physical thermal effects in piezoelectric materials. Compared to the existing one, the model developed in this work considers other features that could be important for the thermal study of BAW SMR. It gives a good estimation of the device maximum temperature versus the dissipated power while keeping a simple calculation method. Moreover, it enables the assessment of the temperature variation inside the device and the comparison of different SMR technologies from a thermal point of view. The obtained results are compared to the experimental measurement as well as the Finite Elements Analysis results. This model can be also improved by taking into account the lateral diffusivity of the heat in each layer around the SMR. Hence for each layer, a heat diffusion surface is defined and is used instead of the constant area *A*. However, this makes calculations more difficult and reduces the model simplicity which is one of its important advantages. The actual model can be used for the temperature mapping of the whole BAW filter once P_d versus P_{in} and f in each resonator is known. This can be done with Finite Elements Analysis or Advanced Design System (**ADS**) simulations by computing the current and the voltage in each node of the equivalent electric model of the BAW filter. According to the reported results, SiN/SiOC-SMR shows higher temperature than SiO_2/W-SMR for the same dissipated power level. The temperature difference is not so high and the resulting frequency shift does not cause problems for Duplexer applications. However, reliability problems due to the generated thermal stress are more likely in the SiN/SiOC interface than the SiO_2/W interface because of the higher temperature variation and the higher dilatation coefficient mismatch between SiN and SiOC as it can be deduced from *TABLE-1*. The same problem can be encountered probably for the SiOC/Mo interface. From an experimental point of view, the presented result is a first assessment for the thermal characterization of BAW resonators. More accurate determination of T_{max} versus P_d law should be possible if a more appropriate thermal imaging technique that enables to limit the lateral heat diffusion is used. In this context, the Lock-In thermography looks as a promising technique for the thermal investigation of BAW devices. Future work using this technique should give more consistent results since this measurement configuration looks closer to the final device configuration in Duplexers.

VII. ACKNOWLEDGEMENT

Authors would like to thank M. Aid (CEA-Leti) and P. Ancey (STMicroelectronics) for samples providing, C. Billard (CEA-Leti) for characterization support, P. Bar and J-F. Carpentier (STMicroelectronics) for helpful discussions.

VIII. REFERENCES

[1–R. Aigner: MEMS in RF filter applications: thin film BAW Technology, Vol.1, Page(s): 5 - 8 (2005)]

[2– Ivira, B et al.: Self-heating study of bulk acoustic wave resonators under high RF power, Ultrasonics, Ferroelectrics and Frequency Control, IEEE Transactions on Volume 55, Issue 1, Page(s):139 – 147 (2008)]

[3– John D. Larson et al.: Power Handling and Temperature Coefficient Studies in FBAR Duplexers for the 1900 MHz PCS Band Ultrasonics Symposium, IEEE Vol. 1, Page(s): 869 – 874 (2000)]

[4– Ivira, B. et al.: Modeling for temperature compensation and temperature characterizations of BAW resonators at GHz frequencies Ultrasonics, Ferroelectrics and Frequency Control, IEEE Transactions on Volume 55, Issue 2, Page(s):421 – 430 (2008)]

[5– Robert Thalhammer et al. : Ohmic effects in BAW-resonators, IEEE MTT-S International,page(s): 390-393(2006)]

[6–J. Ellä, M. Ylilammi : Modelling of ZnO-based BAWs at high signal levels, Ultrasonics Symposium Proceedings, Page(s): 985 – 988 (2002).]

[7– J. P. Holman, "Heat Transfer", McGraw-Hill Book Company, 6th. Edition, 1986].